Improvement in Subsurface Fatigue Cracks under Airframes Fasteners Detection Using Improved Rotating Giant Magneto-Resistance Magnetometer Head

C. DOLABDJIAN, L. PEREZ, ENSICAEN and University of Caen, Caen Cedex, France
G. WACHÉ, Conforemag Sarl, Avilly Saint Leonard, France

Abstract. Improved Giant MagnetoResistance Magnetometers (IGMRM) offers many advantages for subsurface cracks detection. This paper presents new detection opportunity of fatigue cracks close to fasteners or rivets with an improved rotating head. The latter was developed around an IGMRM and a well design electromagnetic flux focuser. The capabilities of the system for the one to the third aluminum layers (3 to 4 mm thick each) flaw detection will be highlighted. Experimental Electro Discharge Machined (EDM) crack sizes under fasteners are some millimeter long and ≈ 100 µm wide. Currently, results show the ability of the system to detect very easily 7 mm long machined crack near rivet under 6 mm of aluminum. The use of IGMRM as field detector, for improved low frequency response and sensitivity of the device, is discussed. A 2D finite element modeling results of electromagnetic field distribution about this newly designed rotating probe is presented. Also, the complete system configuration is described.

Introduction

Giant Magneto-Resistive (GMR) sensors offer many advantages for electromagnetic inspection of crack in conductive materials. In our previous work, we have shown that Improved GMR Magnetometer (IGMRM) could detect crack up to 10 mm in aluminum alloy test sample [1, 2, 3]. More, these developments were performed in mono element and innovative GEGRI multiple element approach [3].

Some other examples of GMR applications exists: C.Wincheski *et al* from NASA Langley Research Center present a rotating probe system dedicated to the detection of fatigue cracks at fasteners and show the capabilities of the system to detect 1.5 long EDM notches in the 4th aluminum layer (1 mm each) of the airframe lap-splice joint sample [4]; C.Smith *et al* show that GMR sensor arrays with frequency independent sensitivity offers improvements in speed, depth, and resolution in eddy-current testing [5]; O.Hesse *et al* give the usage of Magnetic Field Sensors (AMR or GMR) for Low Frequency Eddy Current Testing compare to classical highly sensitive inductive coils [6].

In the way to pursue our development and to show our sensor performances, we present a new rotating head probe, including IGMRM and associated electromagnetic flux focuser dedicated to simple detection of EDM notches of around millimeters at high subsurface.

This paper is organized as follows. The mains IGMRM characteristics and Eddy Current System, flux focuser and rotating head description are presented in part 1. Section 2 is dedicated to experimental results followed by a general conclusion.

1. Rotating head description

1.1 Sensing element and eddy current system

The sensing element uses Giant Magneto-Resistance in an optimized field feedback loop. Magnetometer is able to measure induced eddy current distribution magnetic field image, more details of the method could be find in [1, 2]. Some of the magnetometer performances were summarized in table 1.

Table 1. IGMRM performances

	Improved GMR magnetometer
Supply voltage	± 12 V
First stage gain output sensitivity	≈ 1,000 V/T
Bandwidth	dc to > 300 kHz
Slew-rate	Theoretical > 160 T/s Measured >37.5 T/s
Total Harmonic Distortion (f = 10 Hz - 1 kHz)	Amplitude : ± 1mT$_{peak}$ < 0.03 %* Theoretical : < 0.001%
Noise spectral density	(5/√f) nT/ √Hz for f < 1 kHz ≈ 50 pT/ √Hz for f > 1 kHz
Dynamic (f = 10 Hz to 1 kHz)	143 to 163 dB/√Hz
Full Scale field range	± 12 mT

We can notice its high dynamic and high slew-rate. These performances are required for the development of new Eddy Current System (ECS) and to compete to the classical highly sensitive induction coils.

Figure 1. Sketch view of eddy current system

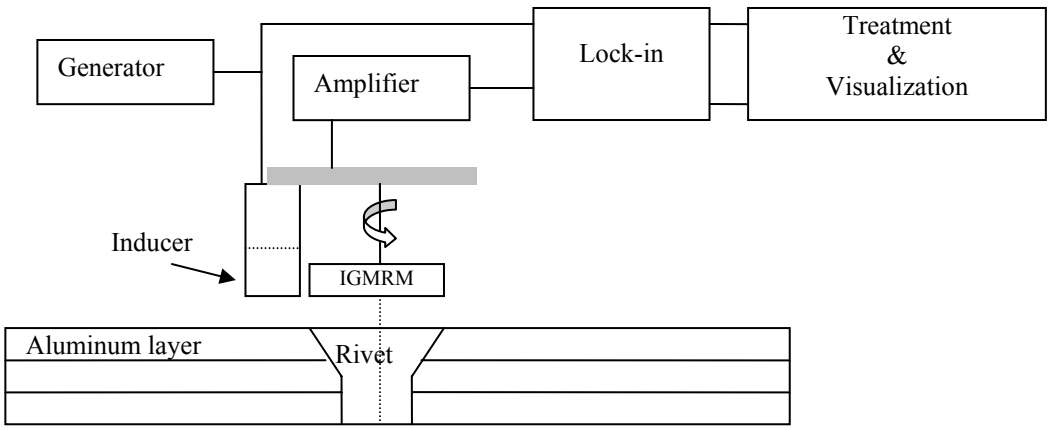

The full eddy current system looks like classical ones. It gives information of the in-phase and out-phase field variations (or amplitude and phase) versus the reference current. A sketch view of the system is presented in figure 1. Its full scale dynamics is around 120 dB/√Hz + 20 log(f_0) to a maximal value of 160 dB/√Hz, where f_0 is the eddy current frequency [3].

1.2 Rotating head description

The rotating experimental head is presented in figure 2. It combines a rotating head contacts and support, an IGMR magnetometer and a "U" flux focuser.

Figure 2. Rotating head view.

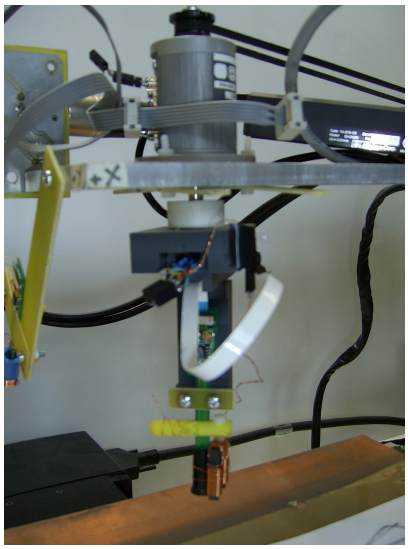

Figure 3. View of the rotating head and associated elements a), top view b).

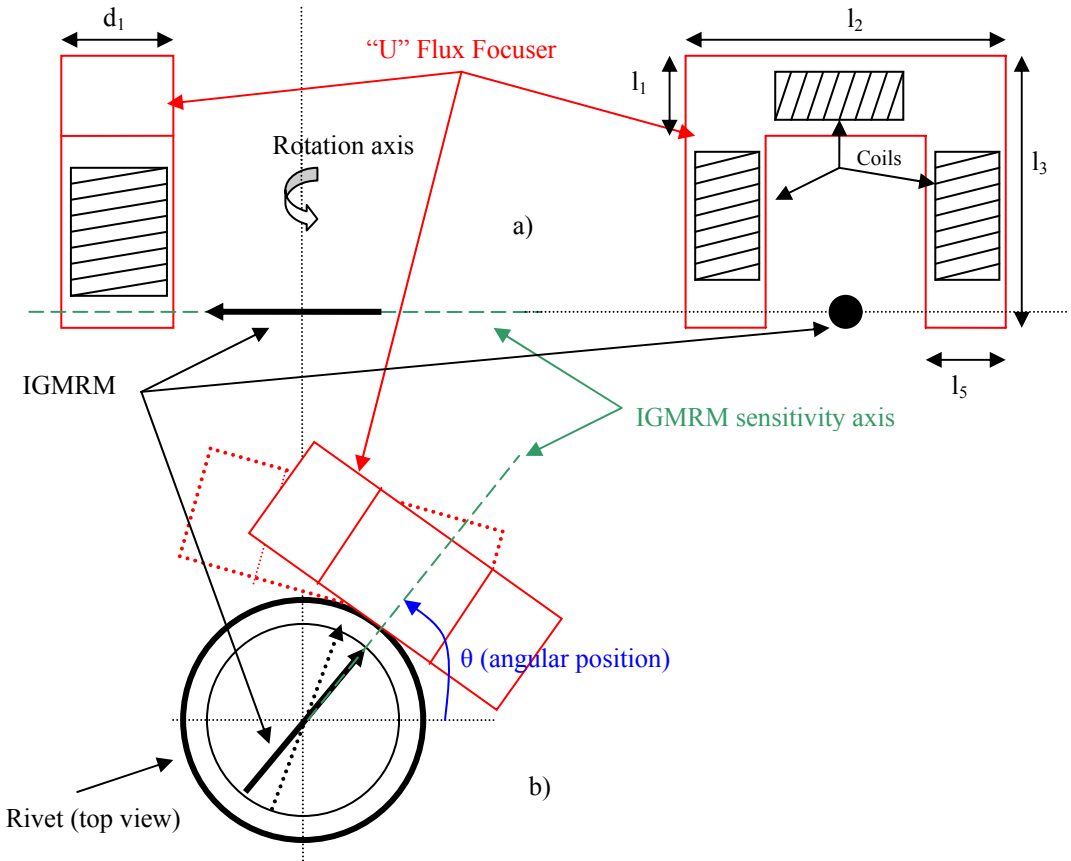

The IGMRM is centered on the axial head rotation. The "U" focuser is placed near the sensing element and is offset to the axial rotation, as given in figure 3.a. Elements are fixed to a rotating support. IGMR sensitivity axis is always directed to the "U" focuser as

named “IGMRM sensitivity axis” in figure 3.b. The rotation head speed is around 0.2 - 1 tr/s. Mostly, the head is positioned at 100 to 500 µm above rivets.

Table 2. “U” Flux focuser characteristics

Geometry	
Size: d_1, l_1, l_2, l_3, l_4, l_5 (mm)	4, 6, 16, 24, 2.5
Coil	
R	3.8
L	≈ 1 mH
Turn number	500

Figure 4. Flux focusing sketch view ($\ell \approx \ell_1 + \ell_2$) a), picture b).

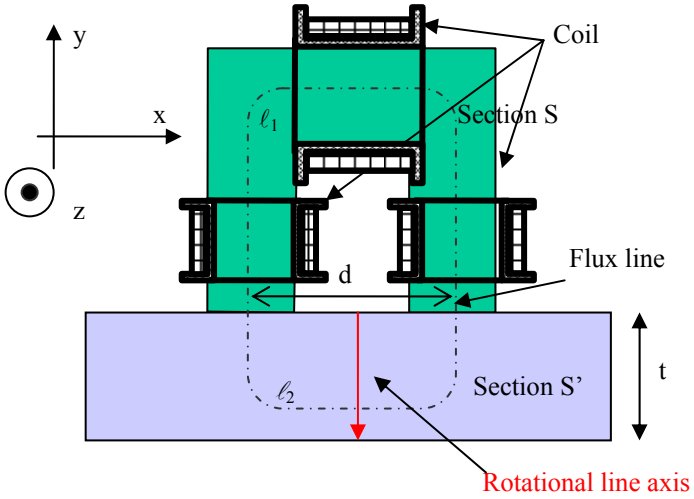

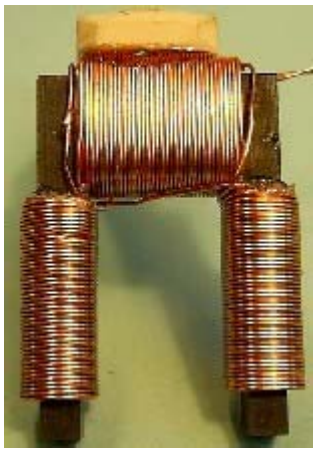

1.3 Flux focuser

We have developed a flux focuser using a soft magnetic core dedicated to concentrate eddy current in subsurface, as presented in figure 4. Sizes and characteristics are resumed in table 2.

It was optimized to increase the current at 10 mm depth. A simple formulation developed with Hopkinson law can help to understand “U” focuser design and performance. Indeed, we can establish that expected magnetic field modulus in non ferromagnetic sample under the U focuser could be given in rough estimation by:

$$|B(y,x)| \approx \frac{\mu_0 \mu_r N I}{\ell \frac{S'}{S} + \pi\delta\left(\mu_r - \frac{S'}{S}\right)} \approx \frac{\mu_0 N I}{\pi\delta} \alpha \frac{cste}{y} \ [T] \qquad (1)$$

where , which depends mainly of the frequency and sample conductivity, is around equal to d/2 or eddy current skin depth considered equivalent in our case, d is geometry dependant size and is simply given by ($d \approx l_2 - l_5$), I is the circulating current coil, N is turn coil number, ℓ is the length of the flux line ($\ell \approx \ell_1 + \ell_2$), μ_r is the U focuser permeability, S the section of the U focuser and S’ is an equivalent sample section. So, we have, in theory, to reduce “d” value to increase the induced current and the head spatial resolution. But, this hypothesis is more accurate near circle of radius (shown in figure 7) and close to sample surface as we can observe in figures 5, 6 and 7. So, (N I) product is the major factor control of eddy current density value at subsurface. A comparison of its simple magnetic field

estimated value to software 2D Finite element modeling simulation (2D COMSOL Multiphysics^{TM}) is presented in figure 5. It shows that equation 1 is around twice of the software simulation result near circle of radius . Meanwhile, higher variations are expected in 3D simulation or experimentally.

Figure 5. Comparison of magnetic field estimated values (eq. 1) to 2D Finite element modeling results for magnetic field density modulus, in 20 mm thick sample aluminum plate, versus depth (in rotational line axis presented in figures 4 and 7).

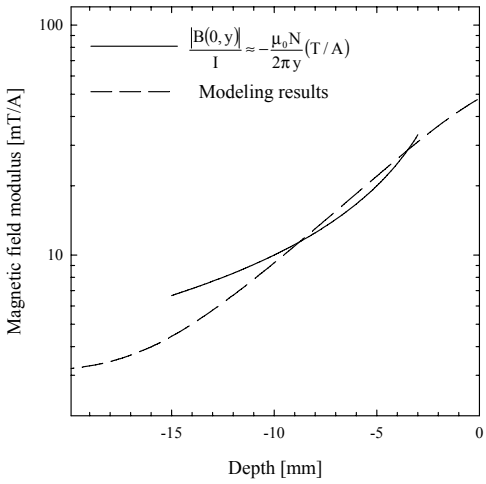

More, the eddy current density evaluation in z axis was made with similar software. Results are given in figure 7 for a 20 mm tick aluminum sample versus depth and in the subsurface given by the rotation line axis presented in figures 4 and 7. The ferromagnetic material permeability is fixed to 5000 and is always working in linear regime. Some 2D views of results are given in figure 7. We expect a current density of around 1 MA/m^2, per ampere of the current coil, at a subsurface of 10 mm. Evaluations are presented in figure 6.

Figure 6. 2D Finite element modeling results for eddy current density in z axis in 20 mm tick sample aluminum plate, versus depth (in rotation line axis presented in figures 4 and 7). Current are induced by focuser at different frequencies a) and for 3 width sizes of the focuser b). Its unit is given in (A/m^2)/A. Indeed, its values are divided by the current coil.

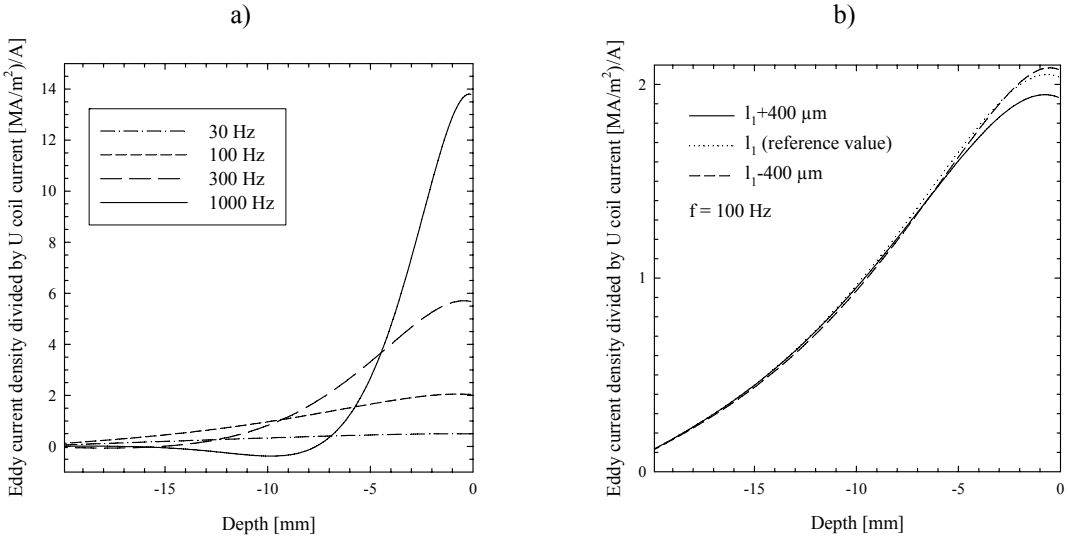

Figure 7. 2D Finite element modeling view (arbitrary color scale) for field induced (Modulus) in U focuser a) and associated eddy current density (z axis) in 20 mm tick sample aluminum b).

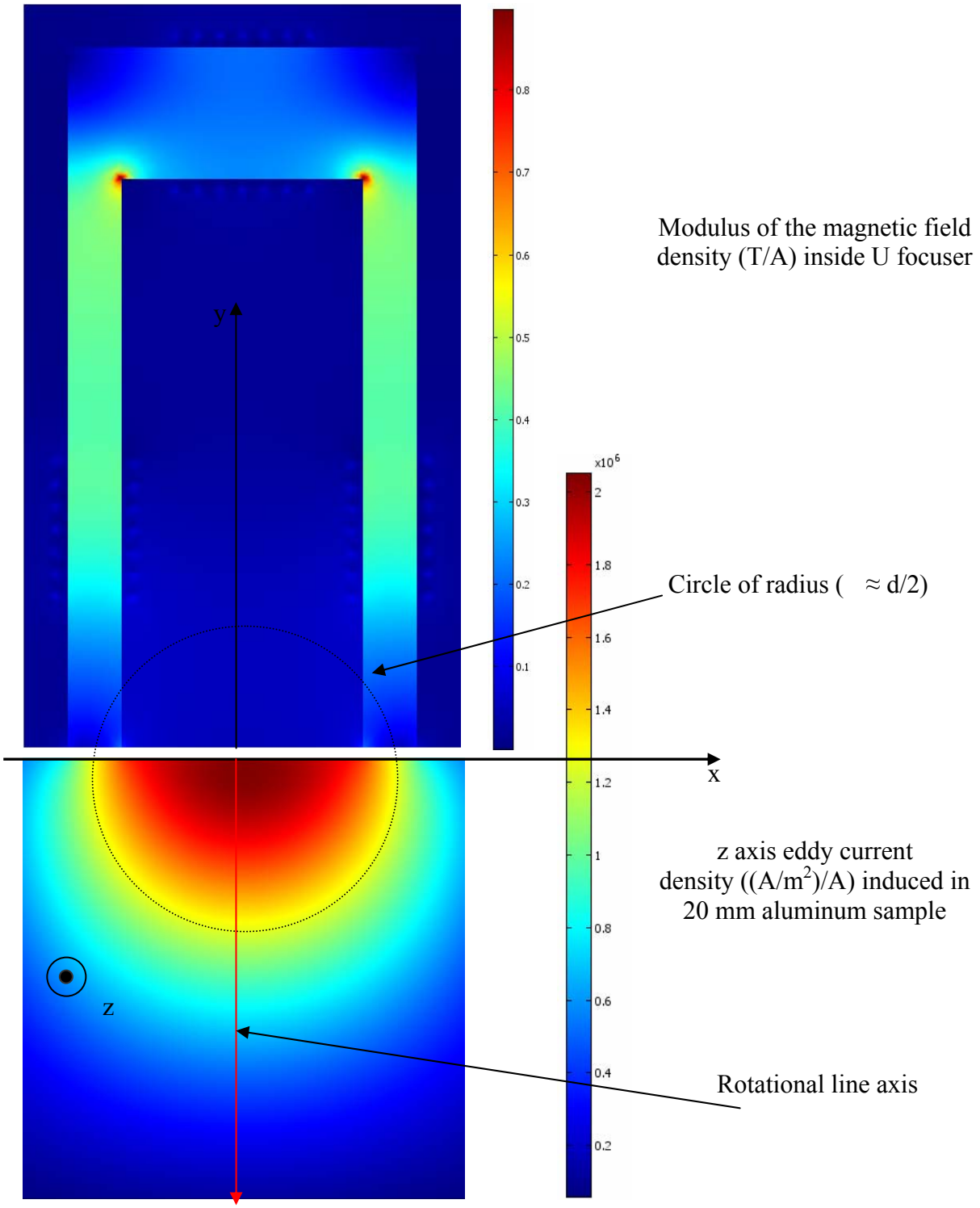

2. Results

An experimental benchmark was developed to asses the feasibility of the improved rotating IGMRM head. Various calibrated fatigue Cracks under Airframes Fasteners were electro discharge machined on an aluminum plate. Multilayer sample consists on 3 layers of 2024

T3 Aluminum (3 mm tick), as shown in figure 8, with 4 mm diameter holes containing ASNA2019/Ti40-15 rivets. Layers 2 and 3 are interchangeable.

In each measurement, we place the rotating head centered on the rivet with a robot and generate its rotation. During the latter, we plot the Lissajous curves of the out-phase versus in phase voltage variations obtained, as given in figure 9.

Figure 8. Sample views: top view a). Cut view EDM placed in second layer b). Cut view with EDM placed in third layer c).

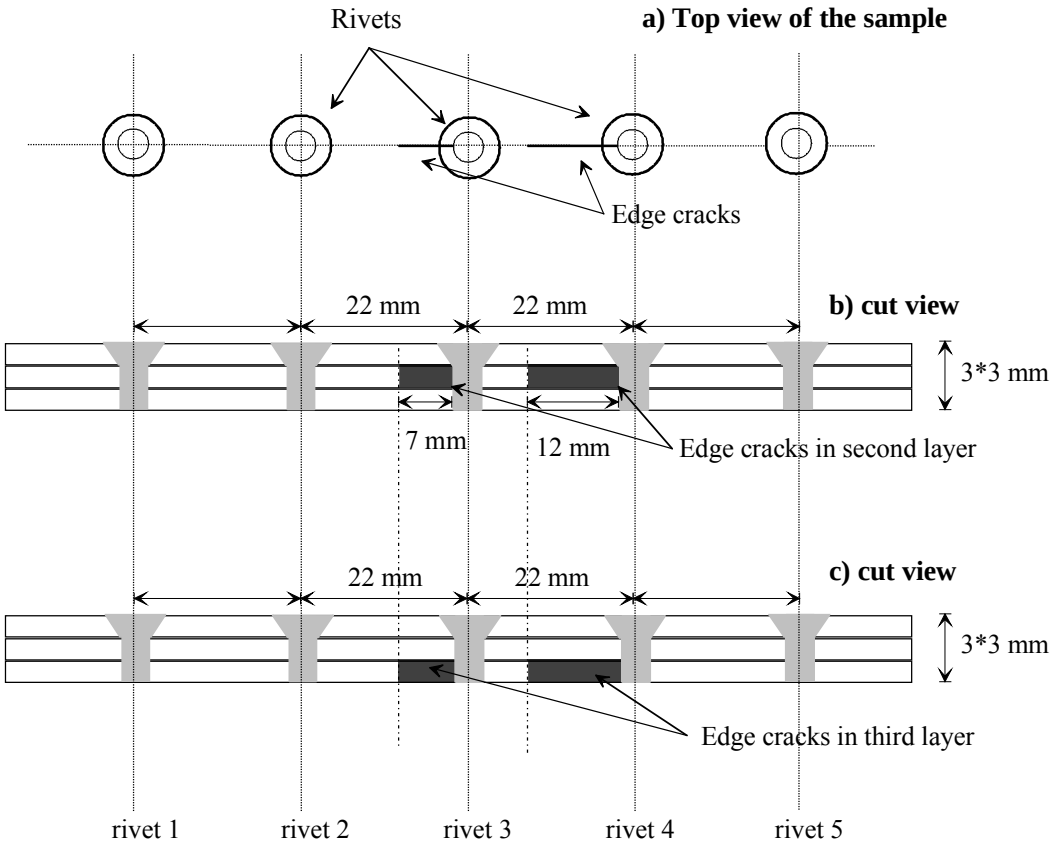

Figure 9. Lissajous curve results (EDM placed in second layer).

Rivet 1	Rivet 2	**Rivet 3 with EDS 7 mm long**	**Rivet 4 with EDS 12 mm long**	Rivet 5
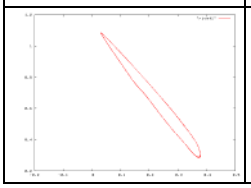	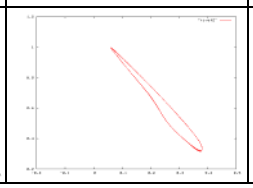	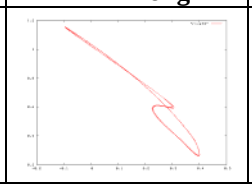	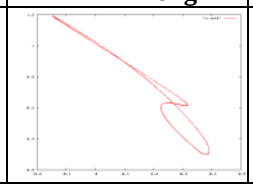	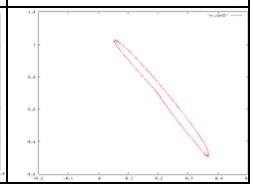

Figure 7. Lissajous curve results (EDM in third layer).

Rivet 1	Rivet 2	**Rivet 3 with EDS 7 mm long**	**Rivet 4 with EDS 12 mm long**	Rivet 5
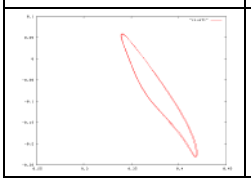	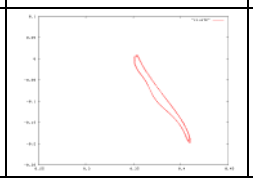	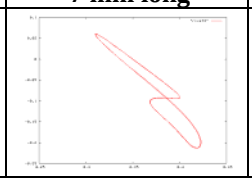	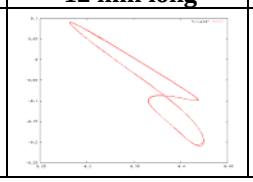	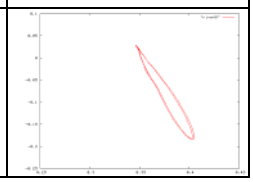

The test found the instrument to have ≈ 100% Probability Of Detection of fatigue cracks, 12 and 7 mm long in the second and third aluminum layers (3 mm tick). Indeed, if we define the POD as:

$$POD = \int_{-10^{\left(\frac{SNR_{dB}}{20}\right)}\sigma}^{10^{\left(\frac{SNR_{dB}}{20}\right)}\sigma} e^{\frac{-x}{2\sigma^2}} \partial x$$

where the SNR is the signal to noise ratio of the equivalent EDM voltage amplitude measurement and ^{2} is the noise variance. In each case of defect detections, the SNR is largely higher than 14 dB. So, it gives a POD greater than 99.9999 %.

3. Conclusion

The detection of fatigue cracks at fasteners holes is always a problem in aging aircraft communities. We show that we are able to detect very easily cracks of 7 mm length below 6 mm of aluminum by using a new Rotating Giant Magneto-Resistance Magnetometer Head. More, this new technique seems to be very accurate and reliable for subsurface crack damage detection. Additional tests will be undertaken to show the technique achievement, crack length detection limit at higher depth and for smaller EDM length.

Acknowledgment

This work was partly supported by European Regional Fund (FEDER) and French National Territories Development Fund (FNADT).

References

[1] L.Perez, C.Dolabdjian, G.Waché, L.Butin, 16th WCNDT'04 Conference, 28 August - 03 September, Montréal (2004)
[2] G.Waché, L.Butin, L.Perez, C.Dolabdjian, Insight - Non-Destructive Testing and Condition Monitoring- The Journal of The British Institute of Non-Destructive Testing - 47(5) - Mai 2005 - Issue
[3] "Investigation in detection of fatigue cracks under rivet head airframe using improved GMR magnetometer in an Eddy Current System", L.Perez, C.Dolabdjian, L.Butin, Jou. of Elec. Eng., 55(10/S), 73-76(2004)
[4] Buzz Wincheski, Min Namkung and Dan Perey, John Simpson and Ed Scales, Richard Louie, Review of Progress in Quantitative NDE,Vol. 21A, AIP, 1007, 2002.
[5] C. H. Smith, R. W. Schneider, T. Dogaru, and S. T. Smith, Review of Progress in Quantitative Nondestructive Evaluation, Vol. 2323, ed. by D. O. Thompson and D. E. Chimenti, (American Institute of Physics, Melville, NY, 2003) pp 406-413
[6] O. Hesse1, S. Pankratyev, MEASUREMENT SCIENCE REVIEW, Volume 5, Section 3, 2005